Exposing and Exploiting Fine-Grained Block Structures for Fast and Accurate Sparse Training

Peng Jiang
The University of Iowa
Iowa City, USA
peng-jiang@uiowa.edu

Lihan Hu
The University of Iowa
Iowa City, USA
lihan-hu@uiowa.edu

Shihui Song
The University of Iowa
Iowa City, USA
shihui-song@uiowa.edu

Abstract

Sparse training is a popular technique to reduce the overhead of training large models. Although previous work has shown promising results for nonstructured sparse models, it is still unclear whether a sparse model with structural constraints can be trained from scratch to high accuracy. In this work, we study the dynamic sparse training for a class of sparse models with shuffled block structures. Compared to nonstructured models, such fine-grained structured models are more hardware-friendly and can effectively accelerate the training process. We propose an algorithm that keeps adapting the sparse model while maintaining the active parameters in shuffled blocks. We conduct experiments on a variety of networks and datasets and obtain positive results. In particular, on ImageNet, we achieve dense accuracy for ResNet50 and ResNet18 at 0.5 sparsity. On CIFAR10/100, we show that dense accuracy can be recovered at 0.6 sparsity for various models. At higher sparsity, our algorithm can still match the accuracy of nonstructured sparse training in most cases, while reducing the training time by up to 5x due to the fine-grained block structures in the models.

1 Introduction

As large neural networks keep advancing the state-of-the-art in many machine learning tasks, training the models has become increasingly expensive. It is reported that training GPT-3 costs an estimated $12 million in computational resources [41]. To reduce the cost, there is a growing interest in developing sparse training algorithms [30, 2, 8, 18, 26, 27]. By computing on a small subset of parameters throughout the training process, these algorithms aim to reduce the memory and computing power consumption for large-scale neural network training.

The existing sparse training methods can be categorized as either static or dynamic. While training a static sparse model from scratch is appealing, it usually requires nontrivial initialization to achieve good accuracy [9, 23, 22]. In contrast, dynamic sparse training uses simple random initialization. In every few iterations, it drops a small number of 'unimportant' weights and replaces them with some new parameters. By exploring a larger set of parameters than the sparse model itself, dynamic sparse training, in general, achieves higher accuracy than static sparse training [14].

Most of the existing dynamic sparse training methods focus on nonstructured models. That is, the active parameters are scattered in the model without any constraints. Although they can retain high accuracy with much fewer parameters, the nonstructured sparse models do not necessarily accelerate the training process because the irregular computation suffers from poor data locality and low parallelism [13, 39]. A common way to improve the efficiency of sparse models is by imposing structures on model parameters. However, current structured models have only been shown attainable by pruning and mostly beneficial to inference [13, 39, 28, 1]. Whether structured models can be obtained by sparse training and in turn accelerate the training process is still an open problem.

36th Conference on Neural Information Processing Systems (NeurIPS 2022).

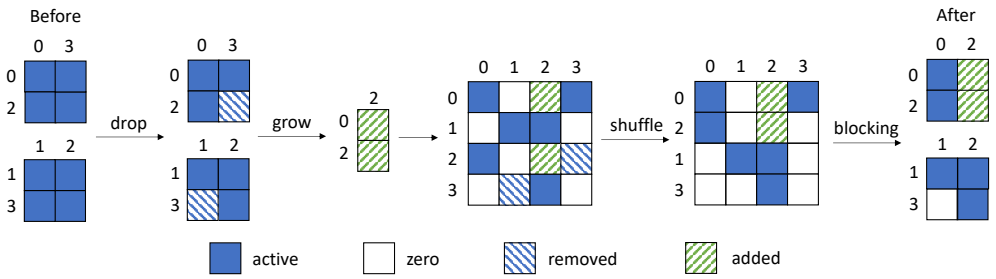

Figure 1: Model adaptation in shuffled-block dynamic sparse training: The active weights are organized in shuffled blocks before adaptation. Any weight can be dropped but new weights must be added in blocks. The new model is reorganized to ensure that all active weights are in shuffled blocks after adaptation.

Some recent work has explored *fine-grained structures* in sparse models for efficient training. For example, Hubara *et al.* [17] propose a method to find N:M transposable sparsity that can benefit both the forward and backward pass. However, their method relies on specialized hardware (sparse tensor cores). Chen *et al.* [3] test the lottery ticket hypothesis [9] for sparse models with shuffled block structures. Although they show promising results that such semi-structured models can be trained to high accuracy from scratch, how to generate a winning ticket without dense training remains unclear.

In this work, we take a step forward and investigate the existence of fine-grained block structures in sparse models with dynamic sparse training. Our idea is illustrated in Fig. 1. We first initialize a sparse model and group the parameters in shuffled blocks. Since the shuffled blocks and their transposes can be efficiently processed by hardware, our method accelerates both the forward and backward pass. In every few iterations, we adapt the model by dropping the smallest weights and adding back the same number of new parameters. Different from previous work which selects new parameters based on dense gradients [8] or dense weights [18], we select blocks of new parameters directly based on the input value and output gradient of each layer, making our algorithm purely sparse. The adapted model is shuffled and blocked again to ensure that the active weights are always organized in shuffled blocks.

We test our algorithm on a variety of networks and datasets and answer the following questions:

1. *Can a randomly initialized sparse model with fine-grained block structures be trained to high accuracy?* We train a ResNet18 and a ResNet50 of 0.5 sparsity with parameters constrained in shuffled blocks of size 16×16 on the ImageNet dataset, and we recover the accuracy of dense models. When the sparsity increases to 0.75, the accuracy drops slightly but still matches the accuracy of nonstructured models with dynamic sparse training. The result is further validated with various models on the CIFAR10/100 dataset.

2. *Does the model adaptation of dynamic sparse training help improve the accuracy of sparse models with fined-grained block structures?* We train sparse models with parameters in shuffled blocks with and without model adaptation. For ResNet18 and ResNet50 on ImageNet, the dynamic approach achieves more than 1% higher accuracy than static training. For different models on CIFAR10/100, dynamic training also achieves higher accuracy than static training, and the improvement is more noticeable when the sparsity is higher.

3. *What is the tradeoff between accuracy and hardware efficiency with different block sizes?* We train sparse models with different block sizes on CIFAR10/100. As expected, models with smaller block structures achieve higher accuracy. We find that the accuracy difference is small for block size 4, 8, 16 and is more noticeable for block size 32. The sparse operations on blocks of size 16×16 can be more than 3x faster than on blocks of size 4×4, but the performance improvement is small when the block size increases to 32. This suggests that block size 16 can achieve a good tradeoff between accuracy and efficiency.

To the best of our knowledge, our work is the first to apply shuffled blocking of model parameters to dynamic sparse training. We believe that our findings can inspire future research on designing hardware-efficient sparse training algorithms.

2 Related Work

Neural network pruning. The conflict between the ever-increasing size of neural networks and the limited computing capacity of hardware has inspired a lot of research on neural network pruning. Early works include [11, 10, 42, 35], in which iterative and heuristic pruning methods with limited and nonstructured sparsity were proposed. These works focus on reducing the size of neural networks but do not consider their performance carefully. The performance issue with nonstructured pruning is later identified in [40], where the authors propose to prune the entire input or output channels so that they can be easily accelerated on CPU and GPU. The downside of these structured pruning methods is that they suffer from notable accuracy loss when sparsity increases. To combine the benefits of structured and nonstructured pruning, hybrid pruning strategies have been proposed. Ma *et al.* propose pattern-based kernel pruning [29] for convolutional neural networks. The convolution kernels can only be pruned to one of several pre-defined patterns so that the pruned model contains some regular structures. Zhu *et al.* propose vector-wise pruning [45]. They divide the weight matrix into fixed-size vectors and keep the top-K elements in each vector. In addition to vector-wise pruning, the authors also adapt the tensor core architecture on GPUs to sparse tensor core in order to support the efficient execution of their vector-wise pruned models. Rumi *et al.* propose the first fine-grained block-structured pruning method for convolutional neural networks [36]. They reorder the convolution kernel matrix with a hypergraph partitioning procedure and group the nonzero weights into a number of shuffled blocks. The authors also provide a CUDA implementation of the shuffled-block-based convolution operation, and show its performance advantage over nonstructured sparse models and dense models on GPU. Recently, the shuffled blocking technique is extended for exploiting dense tensor cores on GPU to further accelerate the computation [16]. Some structured pruning methods can also reduce the computation in each iteration of the training process. However, these methods usually require much more training iterations to recover accuracy. For example, Hrank [24] prunes the convolution layers one-by-one and needs to fine-tune the model for 30 epochs after every layer is pruned. ABCPruner [25] performs end-to-end fine-tuning, but it needs to run the entire training process for multiple cycles. ResRep [7] avoids fine-tuning, but it needs to add extra "compactor" parameters for selecting the channels, resulting in extra computation in each iteration. Moreover, these structured pruning methods require a pre-trained model as input.

Sparse training. Pruning generates sparse models that are fast for inference; however, it does not accelerate the training process. In fact, pruning often needs to be conducted iteratively and increases the training overhead. As neural networks keep growing larger and training becomes prohibitively expensive, people start to be interested in exploiting sparsity to reduce the training cost. Mocanu *et al.* propose the first dynamic sparse training algorithm, Sparse Evolutionary Training (SET), which starts training with a randomly initialized sparse model, prunes weights with small magnitude and adds back weights at random periodically [30]. Following SET, Bellec *et al.* propose Deep Rewiring which augments traditional stochastic gradient descent with a random walk in parameter space [2]. Mostafa *et al.* propose Dynamic Sparse Reparameterization (DSR) which allows the parameter budget to shift between different layers [31]. Dettmers *et al.* propose Sparse Networks from Scratch (SNFS) which uses the momentum of each parameter as the criterion for growing weights [5]. Evci *et al.* point out that all these algorithms can be expressed with a drop-and-grow framework and propose RigL which uses the gradient magnitude as the grow criterion [8]. An issue with RigL is that it needs to compute the full gradient every few iterations, which may not be affordable for large models. Top-kast addresses this issue by maintaining all the weights but computing gradients on a small subset of weights in each iteration. Although these sparse training algorithms show promising results, they still have an accuracy gap with pruning methods. Recently, researchers show that this gap can be closed by using a small batchsize and training for more iterations [26] or by interleaving sparse training with dense training phases [34]. Besides dynamic sparse training, there has been a line of research on static sparse training. Lee *et al.* propose Single-Shot Network Pruning (SNIP) which finds an initial mask with one-shot pruning and keeps the sparse model fixed during training [23]. In a follow-up paper, they refine their initialization method from a signal propagation perspective [22]. Frankle *et al.* propose the Lottery Ticket Hypothesis (LTH) which states that a sparse model can be trained to match the accuracy of the dense model if a good initialization is provided [9]. While appealing, the effectiveness of LTH in reducing the training cost is still unclear as obtaining the "winning ticket" is usually nontrivial [44, 9].

Most of the existing sparse training algorithms (either static or dynamic) focus on nonstructured sparse models. Although they reduce the number of floating-point operations, these models cannot

run efficiently on hardware due to their irregular memory access patterns and limited parallelism. This puts the practicality of sparse training algorithms into doubt. Inspired by the hybrid pruning methods, researchers have worked on extracting fine-grained structures in sparse models to accelerate training. Hubara *et al.* propose a method to find N:M transposable sparsity [17]. Their method accelerates both the forward and backward pass in training and can be used in either a static or dynamic fashion. However, the N:M sparsity relies on specialized hardware (sparse tensor cores on GPU) to deliver good performance and thus is not generally applicable to other hardware or even older GPUs. Chen *et al.* [3] adopt the shuffled blocking technique from [36] and show that a sparse model with shuffled block structures can be trained to dense accuracy at a nontrivial sparsity ratio. However, they need to pre-train a dense model to obtain an initialization for the sparse training. Dietrich *et al.* [6] propose a dynamic sparse training algorithm with block sparsity. However, as we show in §5 and experiments, block sparsity without row/column shuffling has a very low mask diversity and achieves low model accuracy.

3 Preliminaries

Notation. Throughout the paper, we use $W \in \mathbb{R}^{R \times C}$ to denote the parameters in a layer. Here, R is the output channel size; C is the input channel size (if it is a linear layer), or the input channel size times the convolution kernel size (if it is a convolutional layer). We use $In \in \mathbb{R}^{C \times B}$ to denote the input and $Out \in \mathbb{R}^{R \times B}$ to denote the output, where B is the batch size. The gradient w.r.t. W is dW and has the same dimension as W. The element at row i and column j of dW is denoted as dW_{ij}. The gradient w.r.t the output is $dOut$, and the gradient w.r.t. the input is dIn. We use $||\cdot||$ to denote the ℓ_1 norm of a matrix and use $|\cdot|$ to denote the absolute value of each element in a matrix or vector.

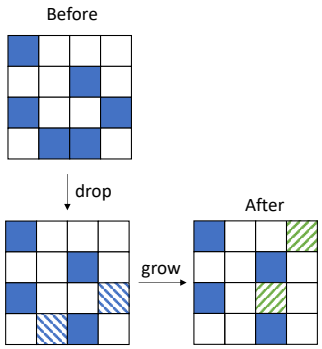

Model adaptation

Algorithm 1: Dynamic sparse training

Input : Network: f_W, Dataset: D, Sparsity distribution: $\mathbb{S} = \{s_1, \ldots, s_l\}$, Update schedule: ΔT, T_{end}

$W \leftarrow$ Randomly sparsify model parameters using $\mathbb{S}$;

for *each training step* t **do**

  Sample a batch $B_t \sim D$;

  $L_t = \sum_{i \in B_t} L(f_W(x_i), y_i)$;

  if $t \mod \Delta T == 0$ **and** $t < T_{end}$ **then**

    for *each layer* l **do**

      $k \leftarrow$ Decide drop number;

      $\mathbb{I}_{drop} \leftarrow$ Select k weights to drop;

      $\mathbb{I}_{grow} \leftarrow$ Select k new weights to grow;

      $W \leftarrow$ Update active weights using $\mathbb{I}_{drop}$ and $\mathbb{I}_{grow}$;

  else $W = W - \alpha \nabla_W L_t$;

Figure 3: Dynamic sparse training with drop-and-grow-based model adaptation.

Dynamic sparse training. Fig. 3 illustrates the idea of dynamic sparse training. The algorithm starts with a randomly initialized sparse model. It adapts the model in every ΔT iterations until iteration T_{end}. The model adaptation involves two operations: *drop* and *grow*. The drop operation discards some weights in the model, and the grow operation adds some new weights back. Different sparse training algorithms use different criteria for the two operations. For example, RigL [8] drops the weights with the smallest magnitudes and grows the same amount of weights with the largest gradients. Top-kast [18] maintains a superset of active weights and drops and grows active weights according to their magnitudes. With the periodic model adaptation, dynamic sparse training algorithms can explore more parameters and achieve higher accuracy than static sparse training [27, 26].

Computations in sparse neural networks. Many operations in a dense neural network can be expressed as general matrix multiplications (GEMM). In a sparse model, the computations are sparse matrix multiplications. For example, the training of a linear layer involves three matrix multiplications: 1) in the forward pass, the input is multiplied with the sparse weight matrix to get the output (i.e., $Out = W \cdot In$); 2) in the backward pass, the gradient of loss w.r.t. the input is computed by multiplying the transpose of the sparse weight matrix with the gradient w.r.t. the

Algorithm 2: Forward pass: $Out = W \cdot In$ for a shuffled block of parameters

Input : $W[S_1][S_2]$, $rowidx[S_1]$, $colidx[S_2]$, $In[C][B]$
Output : $Out[R][B]$
$In'[S_2][B] = In[colidx][B]$;
$Out'[S_1][B] = 0$;
for $i = 0$ **to** $S_1 - 1$ **do**
  for $j = 0$ **to** $S_2 - 1$ **do**
    for $k = 0$ **to** $B - 1$ **do**
      $Out'[i][k]$ += $W[i][j] * In'[j][k]$;
$Out[rowidx][B] = Out'$;

Algorithm 3: Backward pass: $dW = dOut \cdot In^T$ for a shuffled block of parameters

input : $rowidx[S_1]$, $colidx[S_2]$, $dOut[R][B]$, $In[C][B]$
output : $dW[S_1][S_2]$
$In'[S_2][B] = In[colidx][B]$;
$dOut'[S_1][B] = dOut[rowidx][B]$;
$dW'[S_1][S_2] = 0$;
for $i = 0$ **to** $S_1 - 1$ **do**
  for $j = 0$ **to** $S_2 - 1$ **do**
    for $k = 0$ **to** $B - 1$ **do**
      $dW'[i][j]$ += $dOut'[i][k] * In'[j][k]$;
  $dW[rowidx][colidx] = dW'$;

output (i.e., $dIn = W^T \cdot dOut$); 3) the gradient of loss w.r.t. the weight is computed by multiplying the gradient w.r.t. the output with the transpose of input (i.e., $dW = dOut \cdot In^T$). The first two operations are sparse-matrix dense-matrix multiplication (SpMM). The last operation is a sampled dense-dense matrix multiplication (SDDMM) because only the gradients for the active weights need to be computed.

Sparse matrix multiplication with shuffled blocks. SpMM and SDDMM were first studied for efficient execution on GPU in the scientific computing domain [15, 19]. They show that the performance bottleneck of the two operations is the irregular access to the input dense matrix, and they propose *adaptive tiling and reordering* techniques to improve the memory access efficiency. While they target large matrices with high sparsity, the reordering and tiling ideas have inspired *shuffled blocking* techniques to accelerate SpMM and SDDMM for smaller matrices with relatively lower sparsity in sparse neural networks [36, 16, 3]. The idea is illustrated in Fig. 4. The nonzeros in the sparse matrix are organized into small blocks. Algorithm 2 shows the implementation of the forward pass for a shuffled block of parameters. Suppose the row indices of the block are $rowidx$ and column indices are $colidx$. The program first loads $In[colidx][B]$ into cache In' and allocates a cache Out' for $Out[rowidx][B]$. Since the values of $In[colidx][B]$ and $Out[rowidx][B]$ are repeatedly accessed in the computation and accessing cache is much faster than main memory, the memory access overhead is reduced. Similarly, Algorithm 3 shows the computation of the gradients for a block of parameters. The program first loads $In[colidx][B]$ and $dOut[rowidx][B]$ into cache and reuses the data in cache throughout the computation. The larger the block size, the more data reuse the program has. The computation can be further accelerated by exploiting the matrix-multiply units in emerging hardware (e.g., tensor cores on Nvidia GPU) [16]. This is why structured sparse models can deliver better performance than nonstructured models that have even fewer parameters.

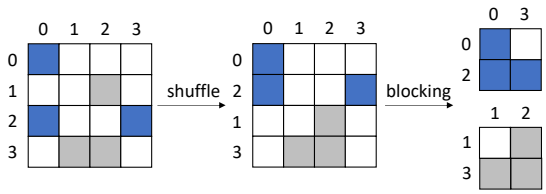

Figure 4: Shuffled blocking a sparse matrix.

4 Proposed Algorithm

As explained in the previous section, for sparse models to run efficiently, it is important to have all the active weights in blocks. Previous work ensures this through pruning [36, 16] or initialization [3]. We now show that sparse models with such fine-grained block structures can also be obtained by dynamic sparse training. Fig. 1 illustrates the model adaptation steps in our algorithm. This section details each of the steps.

Initialization. The algorithm starts with a randomly initialized nonstructured model. We adopt the ERK sparsity distribution [30] to determine the sparsity for each layer. Then, a shuffled blocking procedure is invoked to reshape the sparse model into shuffled blocks.

Shuffled blocking. Suppose N is the number of active weights in a layer and the block size is set to $S_1 \times S_2$. The shuffled blocking procedure aims to put as many active weights into $\lceil N/(S_1 S_2) \rceil$ blocks. As shown in Fig. 4, it first reorders the rows of the sparse matrix so that similar rows are close to each other. The similarity between two rows is defined as the Jaccard similarity of the nonzero columns in the two rows (i.e., the number of common columns divided by the total number of distinct columns). Intuitively, two rows with more common columns have a larger similarity and should be put close to each other. With the definition of similarity between rows, the shuffling of rows can be achieved by a simple clustering procedure. We use the $AgglomerativeClustering$ from sklearn [33] for this task. Since row reordering is performed repeatedly during the training process, we want to keep its overhead as small as possible. We observe that most rows have small similarities with other rows, and reordering them does not improve much of the block density. Therefore, we only cluster the rows that have more than q nonzeros in common columns with other rows, where q (0.2 in our experiments) is a hyperparameter that controls the clustering overhead. After the rows are reordered, we divide them into groups of size S_1. In Fig. 4, S_1 is set to 2, and thus the four rows are divided into two groups: {0,2} and {1,3}. Within each row group, we select S_2 columns to form a block of size $S_1 \times S_2$. To ensure large weights are preserved, we always select the column with the largest ℓ_1 norm in each row group and return the block with the largest ℓ_1 norm among all row groups. This procedure continues until we find enough blocks.

Block-aware drop criterion. The sparse model is adapted in every ΔT iterations. For each layer, we compute the number of weights to be dropped in iteration t with a cosine decaying function:

$$k = \frac{\alpha N}{2}\left(1 + cos\left(\frac{t\pi}{T_{end}}\right)\right) \tag{1}$$

where α is the initial drop ratio and N is the number of active weights in the layer. Following previous dynamic sparse training algorithms [8, 26, 27, 18], we select the k weights with the smallest magnitudes (i.e. $ArgTopK(-|W|, k)$) for removal. Before removing them, we check if these weights make up at least half of the elements in either a row or a column of a block. More specifically, in each shuffled block $\mathcal{B}$, we have the weights to be dropped as $\mathcal{B} \cap ArgTopK(-|W|, k)$. For a weight $w \in \mathcal{B} \cap ArgTopK(-|W|, k)$, the elements in the same row of $\mathcal{B}$ is $\mathcal{B}[rowidx(w), :]$, and the elements in the same column of $\mathcal{B}$ is $\mathcal{B}[:, colidx(w)]$. We remove w if and only if $\mathcal{B}[rowidx(w), :] \cap ArgTopK(-|W|, k)$ has at least $S_1/2$ elements or $\mathcal{B}[:, colidx(w)] \cap ArgTopK(-|W|, k)$ has at least $S_2/2$ elements. If a weight in $ArgTopK(-|W|, k)$ does not have enough other weights to be dropped in the same row/column of a block, the weight will not be dropped. This is because even if we drop it, the weight is very likely to be added back after the blocking procedure. However, because the number of weights to be added in the grow phase is determined by the number of dropped weights, this ineffective dropping of some small weights will result in more new weights being added in the grow phase and may cause more important weights to be discarded by the following shuffled blocking procedure. Our block-aware drop criterion reduces the negative impact of such ineffective drops. Intuitively, when the small weights are concentrated in a few rows or columns, we perform more model adaptation. When the small weights are scattered in many rows and columns, we perform less aggressive adaptation. Fig. 5 shows an example of the block-aware drop criterion. Suppose there are five small weights (marked with diagonal stripes) in a block. Instead of dropping all the five weights, we only drop three of them that are in a row or column with at least two small weights (marked in blue). The two weights with only themselves to be dropped in their rows and columns (marked in orange) will remain active. In our experiments, we find that this block-aware drop criterion is critical for achieving good accuracy for shuffled-block dynamic sparse training (See Appendix A.2).

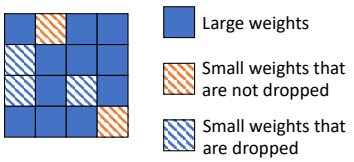

Figure 5: Avoid dropping isolated small weights.

Block-wise grow criterion. The main novelty of our method lies in how we grow the weights. Different from previous work that computes the gradients for all weights and adds the weights with the largest gradients[8, 26, 27], we use $dOut$ and In to estimate the importance of weights. Specifically, since $dW = dOut \cdot In^T$, $dW_{ij} = \langle dOut_i, In_j \rangle$, we have $||dW_{ij}|| \leq ||dOut_i|| \cdot ||In_j||$ where $dOut_i$ represents row i of $dOut$ and In_j represents row j of the input. This suggests that the weights connecting the input channels of larger magnitudes to the output channels of larger gradients are of greater importance. Our grow criterion is designed based on this intuition. Suppose X represents a group of S_x rows in $dOut$ and Y represents a group of S_y rows in In. It is easy to see that XY^T is a shuffled block of size $S_x \times S_y$ in dW. Our goal is to find the blocks of weights with

Table 1: Mask diversity for different sparsity constraints.

Matrix Size ($R \times C$)	8×8			16×16		
Sparsity	1:2	2:4	4:8	1:2	2:4	4:8
Nonstructured	1.8e+18			5.8e+75		
N:M	4.3e+9	2.8e+12	5.8e+14	3.4e+38	6.3e+49	1.1e+59
N:M Transposable	6.6e+4	4.3e+8	1.8e+13	1.8e+19	3.4e+34	9.5e+52
Nonshuffled Block ($S_1 = S_2 = R/4$)	12870					
Nonshuffled Block ($S_1 = S_2 = R/2$)	6					
Shuffled Block ($S_1 = S_2 = R/4$)	1.2e+18			3.7e+48		
Shuffled Block ($S_1 = S_2 = R/2$)	3.1e+11			1.3e+29		

the largest $||XY^T||$. Without computing the actual gradients, we use $||X|| \cdot ||Y^T||$ as an estimate of gradient magnitude. We first sort rows of $dOut$ and In according to their norms in descending order and divide sorted $dOut$ into groups of S_x rows and sorted In into groups of S_y. Then, we compute $||X|| \cdot ||Y^T||$ for the shuffled blocks and select the blocks with largest $||X|| \cdot ||Y^T||$. For a $dOut$ of size $x \times n$ and an input In of size $y \times n$, the FLOPS for computing the norms of rows of $dOut$ and In is $xn + yn$, and the FLOPS for computing the sparse gradients is no more than kn where k is the number of dropped weights in Formula (1). So the total FLOPS with our proposed grow criterion is $xn + yn + kn$. In comparison, the FLOPS for computing dense gradient is xyn. Since k is small, our block-wise grow criterion has a much smaller time complexity than dense gradient computation.

Fig. 6 shows an example of the selection procedure with $S_x = 2$ and $S_y = 1$. Suppose the sorted rows of input are 2, 1, 0, 3, and the sorted rows of $dOut$ are 0, 2, 3, 1. The selection starts from the block in the top left corner (b_0) as it has the largest $||X|| \cdot ||Y^T||$. With b_0 selected, the two blocks (b_1 and b_4) adjacent to b_0 are added to the frontier, and the larger one between the two will be selected in the next step. The selected block may overlap with the existing active blocks. Only the non-overlapping parameters are considered new parameters. We keep selecting new blocks and updating the frontier until new parameters exceed the drop number. In the example of Fig. 1, a block of new parameters ([0,2] and [2,2]) are added. Finally, we reorganize the new model into shuffled blocks. To prevent the new parameters from being discarded by the blocking procedure, we set their value to the maximum value of the active weights. After the new blocks are formed, we reset the value of the new parameters to zero so that they will not affect the output of the network.

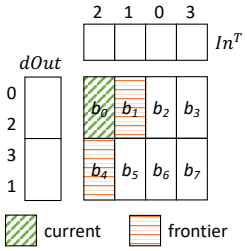

Figure 6: Select new parameters in blocks.

5 Comparison with Transposable N:M Sparsity

Our work is closely related to the line of research that explores fine-grained N:M sparsity in neural networks [43, 17, 38]. While most work focuses on accelerating inference, a recent paper shows that transposable N:M sparsity can be found in sparse models to accelerate both the forward and backward pass in training [17]. This section compares transposable N:M sparsity with shuffled block sparsity.

In [17], the authors propose a measure called *mask diversity* to quantify how much a specific structure constrains the model. Specifically, mask diversity is the total number of distinct sparse masks that satisfy certain sparsity and dimension constraints. They show a positive correlation between the mask diversity and accuracy. We follow their arguments and compute the mask diversity of shuffled block sparsity. For a matrix of size $R \times C$, suppose R and C are divisible by the block size S_1 and S_2, and the sparsity is s. Since the rows are reordered and divided into disjoint groups, the number of ways to choose row groups is $R!/(S_1!)^{R/S_1}$. Once the row groups are fixed, we need to select a total of $RC(1-s)/S_2$ columns from all row groups to form the desired number of blocks. This leads to the following formula for the mask diversity of shuffled block sparsity:

$$MD_{sh_block} = \frac{R!}{(S_1!)^{R/S_1}} \cdot \binom{RC}{RC(1-s)/S_2}. \tag{2}$$

In comparison, the mask diversity of nonshuffled block sparsity is simply choosing $RC(1-s)/(S_1S_2)$ blocks from the total $RC/(S_1S_2)$ blocks. Table 1 lists the mask diversity of shuffled block sparsity

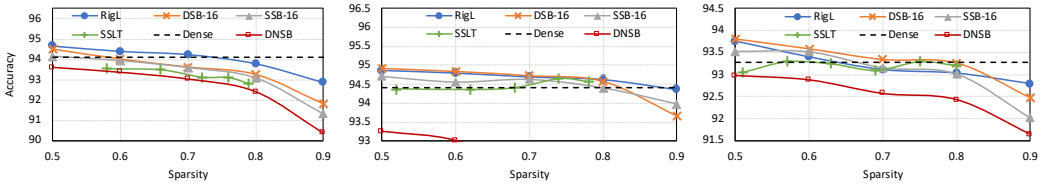

(a) WideResNet22-2 (b) ResNet18 (c) VGG16

Figure 7: Test accuracy (%) over sparsity on CIFAR10.

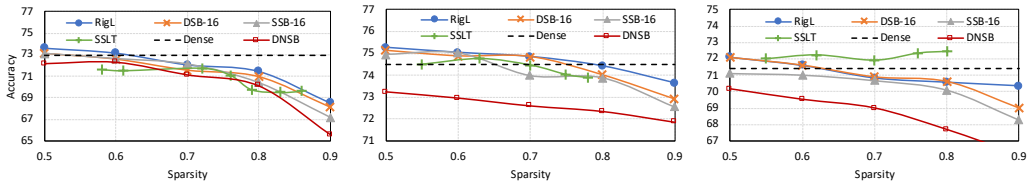

(a) WideResNet22-2 (b) ResNet18 (c) VGG16

Figure 8: Test accuracy (%) over sparsity on CIFAR100.

along with other sparsity constraints for an 8×8 matrix and a 16×16 matrix. The formula for other sparsity constraints can be found in [17]. We can see that nonstructured sparsity has the highest diversity, which explains its superior accuracy to structured sparsity. When the block size is small, shuffled block sparsity has a mask diversity close to nonstructured sparsity. For example, for the 8×8 matrix, when $S_1 = S_2 = R/4 = 2$, the mask diversity is of the same order of magnitude as nonstructured sparsity. When the block size increases, the mask diversity decreases. This illustrates a tradeoff between hardware efficiency and model accuracy for shuffled block sparsity. Compared to N:M sparsity which only benefits the forward pass, shuffled block sparsity benefits both the forward and backward pass and yet has a higher mask diversity when $S_1 = S_2 \leq 4$ and $M = 2$. Compared to N:M transposable sparsity, shuffled block sparsity has a higher mask diversity when $S_1 = S_2 \leq 4$ and $M \leq 4$.

Moreover, N:M sparsity relies on sparse-matrix-multiply units in emerging hardware (sparse tensor cores on Nvidia Ampere GPU) to deliver good performance, whereas shuffled blocking accelerates the computation on traditional computing units and can exploit dense-matrix-multiply units which are more broadly supported by hardware (e.g. dense tensor cores on GPU, AMX on Intel CPU, MMA on IBM Power10 processor). As the current Nvidia GPU only supports sparse tensor cores with $N = 2, M = 4$ and dense tensor cores with $S_1 = S_2 = 4$, shuffled blocking is expected to be a more flexible and more efficient way to accelerate sparse training. We can also see that shuffled block sparsity has a much higher mask diversity than nonshuffled block sparsity. This is because the shuffling of rows and columns significantly increases the number of ways to form nonzero blocks.

6 Experiments

We test our algorithm with ResNet18 and ResNet50 [12] on the ImageNet dataset [4], and WideResNet22-2, ResNet18 and VGG16 [37] on CIFAR10 [20] and CIFAR100 dataset [21]. For

Table 2: Top-1 accuracy on ImageNet. DSB represents our Dynamic Shuffled Block training, and SSB represents Static Shuffled Block training with random initialization. The number before DSB and SSB indicates sparsity, and the number after DSB and SSB is the block size. SSLT represents Structured Sparse Lottery Ticket from [3]. The number before SSLT indicates sparsity. '-' indicates missing data in literature.

Model	Dense	0.5 DSB-16	0.5 SSB-16	0.51 SSLT	0.7 SSLT	0.75 DSB-16	0.75 SSB-16	0.8 RigL
ResNet50	76.13	**76.33**	75.83	75.65	71.5	74.04	72.76	75.1
ResNet18	69.76	**69.84**	68.52	-		65.72	64.49	-

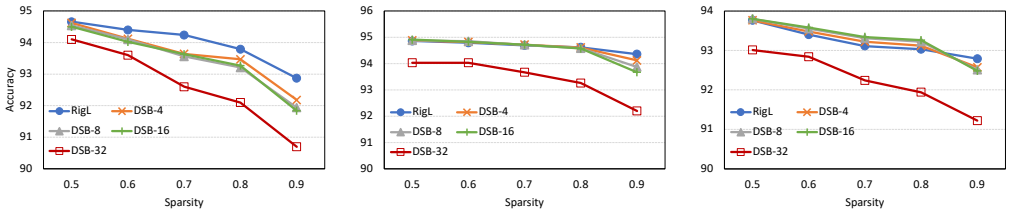

(a) WideResNet22-2 (b) ResNet18 (c) VGG16

Figure 9: Test accuracy (%) over sparsity on CIFAR-10 with DSB using different block sizes. RigL corresponds to DSB using block size 1.

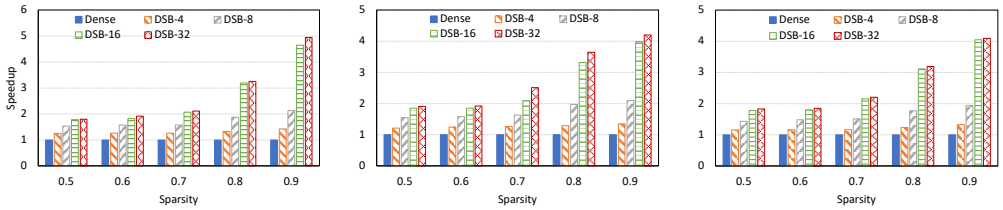

(a) WideResNet22-2 (b) ResNet18 (c) VGG16

Figure 10: Average speedup of sparse convolution over dense convolution operations on CIFAR10.

ImageNet, the models are trained for 100 epochs with batch size 256. The learning rate schedule starts with a linear warm up reaching its maximum value of 0.1 at epoch 5 which is then dropped by a factor of 10 at epochs 30, 70, 90. For CIFAR10/100, the models are trained for 250 epochs with batch size 128. The learning rate is initialized to 0.1 and is decreased by a factor of 5 every 30,000 iterations. The standard SGD with a momentum of 0.9 is used as the optimizer. For dynamic sparse training, the initial drop ratio α is set to 0.3, ΔT is set to 1600 for ImageNet and 100 for CIFAR10/100, and T_{end} is set to 400000 for ImageNet and 75000 for CIFAR10/100.

Accuracy compared with other training methods. Table 2 lists the top-1 accuracy of ResNet18 and ResNet50 trained with different methods on ImageNet. Our dynamic shuffled block training (DSB) recovers the accuracy of the dense models at 0.5 sparsity. In comparison, the structured sparse lottery ticket (SSLT) [3] has a slight accuracy drop for ResNet50 at 0.51 sparsity while requiring a dense pre-training for initializing the sparse mask. The accuracy of DSB at sparsity 0.75 is also higher than that of SSLT at sparsity 0.7. Fig. 7 shows the test accuracy of WideResNet22-2, ResNet18 and VGG16 trained with different methods on CIFAR10. All the experiments are run five times. The accuracies plotted in the figures are the average values. The difference in accuracy between different runs is smaller than 0.05%. We can see that our DSB recovers dense accuracy at 0.5 and 0.6 sparsity for all three models. In contrast, SSLT has a noticeable accuracy drop for WideResNet22 and ResNet18 (although they can achieve dense accuracy at lower sparsities [3]). Compared with nonstructured dynamic sparse training (RigL [8]), our DSB has slightly lower accuracy at 0.5 and 0.6 sparsity, and the accuracy gap widens as the sparsity gets higher. Fig. 8 shows the test accuracy on CIFAR100. Again, our DSB recovers dense accuracy at 0.5 and 0.6 sparsity. For WideResNet22-2 and ResNet18, our DSB achieves slightly higher accuracy than SSLT at small sparsity (≤ 0.7) and almost the same accuracy at higher sparsity (> 0.7). For VGG16, SSLT achieves surprisingly higher accuracy than both dense training and our DSB, but they require a dense pre-training for initialization. For all the test cases, nonshuffled block sparsity (DNSB) achieves apparently lower accuracies than other methods, which is consistent with the mask diversity shown in Table 1.

Importance of model adaptation. The results in Table 2 and Fig. 7 and 8 also show that the model adaptation is critical to the accuracy of sparse training. For ResNet50 and ResNet18 on ImageNet, without model adaptation, static shuffled block training (SSB) cannot recover dense accuracy at 0.5 sparsity. Its accuracy at 0.75 sparsity is more than 1% lower than DSB. For WideResNet22-2, ResNet18, and VGG16 on CIFAR10/100, SSB also has lower accuracy than DSB, and the accuracy gap is larger at higher sparsity.

Tradeoff between accuracy and efficiency with different block sizes. To show the effects of block size on accuracy, we run DSB with different block sizes. The results are shown in Fig. 9. DSB-4,8,16 achieve almost the same accuracy when sparsity ≤ 0.8. DSB-4 shows a slight advantage over DSB-8,16 at 0.9 sparsity. When the block size increases to 32, we observe an apparent accuracy drop, and the drop is more significant at higher sparsity. To show the effects of block size on performance, we test the implementation of shuffled block convolution from [36] on an Nvidia RTX3090 GPU. Fig. 10 shows the average speedups of shuffled block convolution with different block sizes over dense convolution. We can see that when the block size is small, the sparse convolution has almost no performance advantage over dense convolution, even at a high sparsity. As the block size increases, the shuffled block convolution achieves better performance. Notably, when the block size increases from 8 to 16, the sparse computation achieves the largest marginal speedups. When the block size increases from 16 to 32, the performance improvement is small. This is because the convolution operation with 16×16 blocks already saturates the cache on the GPU platform. The results suggest that block size 16 achieves a good tradeoff between the accuracy and efficiency of DSB.

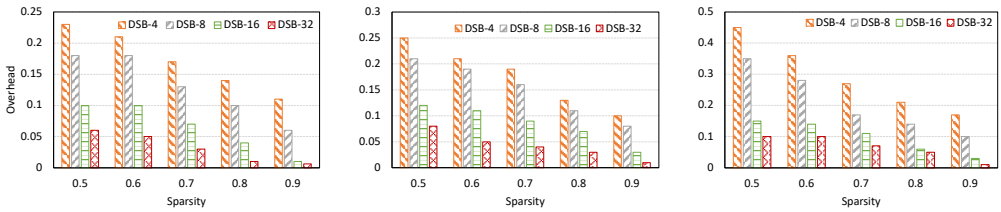

(a) WideResNet22-2 (b) ResNet18 (c) VGG16

Figure 11: The ratio of shuffled blocking time to dense training time for different models on CIFAR10.

Overhead of shuffled blocking. Although shuffled blocking is an expensive operation, it is performed only once in every ΔT iterations. Fig. 11 shows the overhead of shuffled blocking. The execution time of shuffled blocking accounts for 1% to 45% of total training time. We can see that, as the sparsity increases, the overhead of shuffled blocking decreases. As the block size increases, the number of blocks decreases, and the overhead also decreases. When block size is set to 16, the shuffled blocking procedure takes about 10% of the total training time. According to the speedups in Fig. 10, the overhead can be justified by the performance improvements brought by sparse computation.

7 Conclusion

We propose a dynamic sparse training algorithm that extracts and exploits fine-grained block structures in sparse models. Our algorithm is designed based on the drop-and-grow model adaptation framework and features a block-aware drop criterion and a block-wise grow criterion. We show that a randomly initialized sparse model with shuffled block structures can be trained to high accuracy, and the training process can be effectively accelerated.

References

[1] Brian Bartoldson, Ari Morcos, Adrian Barbu, and Gordon Erlebacher. The generalization-stability tradeoff in neural network pruning. *Advances in Neural Information Processing Systems*, 33:20852–20864, 2020.

[2] Guillaume Bellec, David Kappel, Wolfgang Maass, and Robert Legenstein. Deep rewiring: Training very sparse deep networks. *arXiv preprint arXiv:1711.05136*, 2017.

[3] Tianlong Chen, Xuxi Chen, Xiaolong Ma, Yanzhi Wang, and Zhangyang Wang. Coarsening the granularity: Towards structurally sparse lottery tickets. *arXiv preprint arXiv:2202.04736*, 2022.

[4] Jia Deng, Wei Dong, Richard Socher, Li-Jia Li, Kai Li, and Li Fei-Fei. Imagenet: A large-scale hierarchical image database. In *2009 IEEE conference on computer vision and pattern recognition*, pages 248–255. Ieee, 2009.

[5] Tim Dettmers and Luke Zettlemoyer. Sparse networks from scratch: Faster training without losing performance. *arXiv preprint arXiv:1907.04840*, 2019.

[6] Anastasia Dietrich, Frithjof Gressmann, Douglas Orr, Ivan Chelombiev, Daniel Justus, and Carlo Luschi. Towards structured dynamic sparse pre-training of bert. *arXiv preprint arXiv:2108.06277*, 2021.

[7] Xiaohan Ding, Tianxiang Hao, Jianchao Tan, Ji Liu, Jungong Han, Yuchen Guo, and Guiguang Ding. Resrep: Lossless cnn pruning via decoupling remembering and forgetting. In *Proceedings of the IEEE/CVF International Conference on Computer Vision*, pages 4510–4520, 2021.

[8] Utku Evci, Trevor Gale, Jacob Menick, Pablo Samuel Castro, and Erich Elsen. Rigging the lottery: Making all tickets winners. In *International Conference on Machine Learning*, pages 2943–2952. PMLR, 2020.

[9] Jonathan Frankle and Michael Carbin. The lottery ticket hypothesis: Finding sparse, trainable neural networks. In *International Conference on Learning Representations*, 2019.

[10] Song Han, Huizi Mao, and William J Dally. Deep compression: Compressing deep neural networks with pruning, trained quantization and huffman coding. *arXiv preprint arXiv:1510.00149*, 2015.

[11] Song Han, Jeff Pool, John Tran, and William J. Dally. Learning both weights and connections for efficient neural networks. In *Proceedings of the 28th International Conference on Neural Information Processing Systems - Volume 1*, NIPS'15, pages 1135–1143, Cambridge, MA, USA, 2015. MIT Press.

[12] Kaiming He, Xiangyu Zhang, Shaoqing Ren, and Jian Sun. Deep residual learning for image recognition. In *Proceedings of the IEEE conference on computer vision and pattern recognition*, pages 770–778, 2016.

[13] Yihui He, Xiangyu Zhang, and Jian Sun. Channel pruning for accelerating very deep neural networks. In *Proceedings of the IEEE international conference on computer vision*, pages 1389–1397, 2017.

[14] Torsten Hoefler, Dan Alistarh, Tal Ben-Nun, Nikoli Dryden, and Alexandra Peste. Sparsity in deep learning: Pruning and growth for efficient inference and training in neural networks. *Journal of Machine Learning Research*, 22(241):1–124, 2021.

[15] Changwan Hong, Aravind Sukumaran-Rajam, Israt Nisa, Kunal Singh, and P Sadayappan. Adaptive sparse tiling for sparse matrix multiplication. In *Proceedings of the 24th Symposium on Principles and Practice of Parallel Programming*, pages 300–314, 2019.

[16] Guyue Huang, Haoran Li, Minghai Qin, Fei Sun, Yufei Ding, and Yuan Xie. Shfl-bw: Accelerating deep neural network inference with tensor-core aware weight pruning. *arXiv preprint arXiv:2203.05016*, 2022.

[17] Itay Hubara, Brian Chmiel, Moshe Island, Ron Banner, Joseph Naor, and Daniel Soudry. Accelerated sparse neural training: A provable and efficient method to find n: m transposable masks. *Advances in Neural Information Processing Systems*, 34, 2021.

[18] Siddhant Jayakumar, Razvan Pascanu, Jack Rae, Simon Osindero, and Erich Elsen. Top-kast: Top-k always sparse training. *Advances in Neural Information Processing Systems*, 33:20744–20754, 2020.

[19] Peng Jiang, Changwan Hong, and Gagan Agrawal. A novel data transformation and execution strategy for accelerating sparse matrix multiplication on gpus. In *Proceedings of the 25th ACM SIGPLAN Symposium on Principles and Practice of Parallel Programming*, pages 376–388, 2020.

[20] Alex Krizhevsky, Vinod Nair, and Geoffrey Hinton. Cifar-10 (canadian institute for advanced research).

[21] Alex Krizhevsky, Vinod Nair, and Geoffrey Hinton. Cifar-100 (canadian institute for advanced research).

[22] Namhoon Lee, Thalaiyasingam Ajanthan, Stephen Gould, and Philip HS Torr. A signal propagation perspective for pruning neural networks at initialization. *arXiv preprint arXiv:1906.06307*, 2019.

[23] Namhoon Lee, Thalaiyasingam Ajanthan, and Philip HS Torr. Snip: Single-shot network pruning based on connection sensitivity. *arXiv preprint arXiv:1810.02340*, 2018.

[24] Mingbao Lin, Rongrong Ji, Yan Wang, Yichen Zhang, Baochang Zhang, Yonghong Tian, and Ling Shao. Hrank: Filter pruning using high-rank feature map. In *Proceedings of the IEEE/CVF conference on computer vision and pattern recognition*, pages 1529–1538, 2020.

[25] Mingbao Lin, Rongrong Ji, Yuxin Zhang, Baochang Zhang, Yongjian Wu, and Yonghong Tian. Channel pruning via automatic structure search. In Christian Bessiere, editor, *Proceedings of the Twenty-Ninth International Joint Conference on Artificial Intelligence, IJCAI-20*, pages 673–679. International Joint Conferences on Artificial Intelligence Organization, 7 2020.

[26] Shiwei Liu, Tianlong Chen, Xiaohan Chen, Zahra Atashgahi, Lu Yin, Huanyu Kou, Li Shen, Mykola Pechenizkiy, Zhangyang Wang, and Decebal Constantin Mocanu. Sparse training via boosting pruning plasticity with neuroregeneration. *Advances in Neural Information Processing Systems*, 34, 2021.

[27] Shiwei Liu, Lu Yin, Decebal Constantin Mocanu, and Mykola Pechenizkiy. Do we actually need dense over-parameterization? in-time over-parameterization in sparse training. In *International Conference on Machine Learning*, pages 6989–7000. PMLR, 2021.

[28] Zhuang Liu, Jianguo Li, Zhiqiang Shen, Gao Huang, Shoumeng Yan, and Changshui Zhang. Learning efficient convolutional networks through network slimming. In *Proceedings of the IEEE international conference on computer vision*, pages 2736–2744, 2017.

[29] Xiaolong Ma, Fu-Ming Guo, Wei Niu, Xue Lin, Jian Tang, Kaisheng Ma, Bin Ren, and Yanzhi Wang. Pconv: The missing but desirable sparsity in dnn weight pruning for real-time execution on mobile devices. In *Proceedings of the AAAI Conference on Artificial Intelligence*, volume 34, pages 5117–5124, 2020.

[30] Decebal Constantin Mocanu, Elena Mocanu, Peter Stone, Phuong H Nguyen, Madeleine Gibescu, and Antonio Liotta. Scalable training of artificial neural networks with adaptive sparse connectivity inspired by network science. *Nature communications*, 9(1):1–12, 2018.

[31] Hesham Mostafa and Xin Wang. Parameter efficient training of deep convolutional neural networks by dynamic sparse reparameterization. In *International Conference on Machine Learning*, pages 4646–4655. PMLR, 2019.

[32] Adam Paszke, Sam Gross, Francisco Massa, Adam Lerer, James Bradbury, Gregory Chanan, Trevor Killeen, Zeming Lin, Natalia Gimelshein, Luca Antiga, Alban Desmaison, Andreas Köpf, Edward Z. Yang, Zachary DeVito, Martin Raison, Alykhan Tejani, Sasank Chilamkurthy, Benoit Steiner, Lu Fang, Junjie Bai, and Soumith Chintala. Pytorch: An imperative style, high-performance deep learning library. In Hanna M. Wallach, Hugo Larochelle, Alina Beygelzimer, Florence d'Alché-Buc, Emily B. Fox, and Roman Garnett, editors, *Advances in Neural Information Processing Systems 32: Annual Conference on Neural Information Processing Systems 2019, NeurIPS 2019, December 8-14, 2019, Vancouver, BC, Canada*, pages 8024–8035, 2019.

[33] F. Pedregosa, G. Varoquaux, A. Gramfort, V. Michel, B. Thirion, O. Grisel, M. Blondel, P. Prettenhofer, R. Weiss, V. Dubourg, J. Vanderplas, A. Passos, D. Cournapeau, M. Brucher, M. Perrot, and E. Duchesnay. Scikit-learn: Machine learning in Python. *Journal of Machine Learning Research*, 12:2825–2830, 2011.

[34] Alexandra Peste, Eugenia Iofinova, Adrian Vladu, and Dan Alistarh. Ac/dc: Alternating compressed/decompressed training of deep neural networks. *Advances in Neural Information Processing Systems*, 34, 2021.

[35] Ao Ren, Tianyun Zhang, Shaokai Ye, Jiayu Li, Wenyao Xu, Xuehai Qian, Xue Lin, and Yanzhi Wang. Admm-nn: An algorithm-hardware co-design framework of dnns using alternating direction methods of multipliers. In *Proceedings of the Twenty-Fourth International Conference on Architectural Support for Programming Languages and Operating Systems*, pages 925–938, 2019.

[36] Masuma Akter Rumi, Xiaolong Ma, Yanzhi Wang, and Peng Jiang. Accelerating sparse cnn inference on gpus with performance-aware weight pruning. In *Proceedings of the ACM International Conference on Parallel Architectures and Compilation Techniques*, pages 267–278, 2020.

[37] Karen Simonyan and Andrew Zisserman. Very deep convolutional networks for large-scale image recognition. In *International Conference on Learning Representations*, 2015.

[38] Wei Sun, Aojun Zhou, Sander Stuijk, Rob Wijnhoven, Andrew O Nelson, Henk Corporaal, et al. Dominosearch: Find layer-wise fine-grained n: M sparse schemes from dense neural networks. *Advances in Neural Information Processing Systems*, 34, 2021.

[39] Wei Wen, Chunpeng Wu, Yandan Wang, Yiran Chen, and Hai Li. Learning structured sparsity in deep neural networks. *Advances in neural information processing systems*, 29, 2016.

[40] Wei Wen, Chunpeng Wu, Yandan Wang, Yiran Chen, and Hai Li. Learning structured sparsity in deep neural networks. In *Proceedings of the 30th International Conference on Neural Information Processing Systems*, NIPS'16, pages 2082–2090, USA, 2016. Curran Associates Inc.

[41] Kyle Wiggers. Openai's massive gpt-3 model is impressive, but size isn't everything. url-https://www.theregister.com/2020/11/04/gpt3_carbon_footprint_estimate/, 2020.

[42] Tianyun Zhang, Shaokai Ye, Kaiqi Zhang, Jian Tang, Wujie Wen, Makan Fardad, and Yanzhi Wang. A systematic dnn weight pruning framework using alternating direction method of multipliers. In *ECCV*, 2018.

[43] Aojun Zhou, Yukun Ma, Junnan Zhu, Jianbo Liu, Zhijie Zhang, Kun Yuan, Wenxiu Sun, and Hongsheng Li. Learning n: m fine-grained structured sparse neural networks from scratch. *arXiv preprint arXiv:2102.04010*, 2021.

[44] Hattie Zhou, Janice Lan, Rosanne Liu, and Jason Yosinski. Deconstructing lottery tickets: Zeros, signs, and the supermask. *Advances in neural information processing systems*, 32, 2019.

[45] Maohua Zhu, Tao Zhang, Zhenyu Gu, and Yuan Xie. Sparse tensor core: Algorithm and hardware co-design for vector-wise sparse neural networks on modern gpus. In *Proceedings of the 52nd Annual IEEE/ACM International Symposium on Microarchitecture*, pages 359–371, 2019.

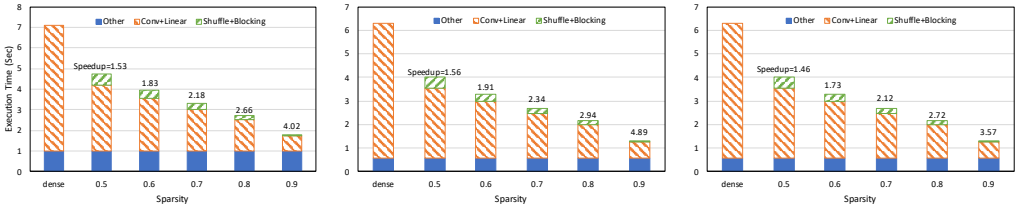

(a) WideResNet22-2 (b) ResNet18 (c) VGG16

Figure 12: Training time per epoch for different models on CIFAR10.

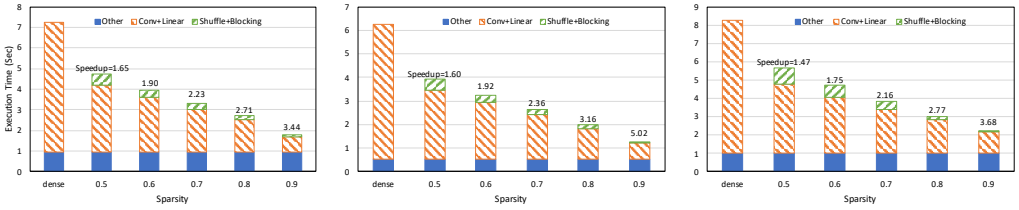

(a) WideResNet22-2 (b) ResNet18 (c) VGG16

Figure 13: Training time per epoch for different models on CIFAR100.

A Appendix

A.1 End-to-end speedups

To show the end-to-end speedups with shuffled-block sparsity, we obtain the layer-wise execution time of dense training on an Nvidia RTX 3090 GPU with PyTorch Profiler [32]. The sparse training time is estimated by replacing the execution time of dense convolution and linear operations with the execution time of shuffled-block convolution and linear operations. Fig. 12 shows the average training time per epoch for WideResNet22-2, ResNet18, and VGG16 on CIFAR10. The batch size is set to 128, and the shuffled block size is set to 16. We can see that convolution and linear operations account for more than 80% execution time of the dense models. Shuffled-block sparse training effectively reduces the execution time of these layers at different sparsities, achieving overall 1.46x to 5.02x speedups. Fig. 13 shows similar speedups for the three models on CIFAR100 dataset.

A.2 Benefits of block-aware drop criterion

Figure 14 shows the accuracy of shuffled-block dynamic sparse training with and without our block-aware drop criterion for WideResNet22-2, ResNet18, and VGG16 on CIFAR10 dataset. As we explain in §4, the original drop criterion leads to ineffective drops of small weights and causes the more important weights to be discarded by the shuffled blocking procedure. The experiments show that the original drop criterion has apparently lower accuracies than our block-aware drop criterion. Fig. 15 shows a similar pattern for the three models on CIFAR100 dataset. The results validate the advantage of our block-aware drop criterion for shuffled-block dynamic sparse training.

A.3 Memory consumption analysis

Table 3 lists the memory consumption of our dynamic shuffled-block training (DSB) and two other dynamic sparse training methods (RigL [8] and Top-KAST [18]). We only compare the memory consumption of model weights and gradients since the intermediate activations are of the same size with different training methods. Suppose the number of parameters in the dense model is N and the density of the sparse model is d ($0 < d \leq 1$). In each training iteration, RigL [8] stores Nd weights and computes their gradients. For model adaptation, RigL needs to compute the gradients for all the N parameters and select the parameters with the largest gradients for growing. Our DSB has the same memory consumption as RigL in each training iteration, but we need not compute the full gradients for model adaptation thanks to our block-wise grow criterion. Top-KAST [18] aims to

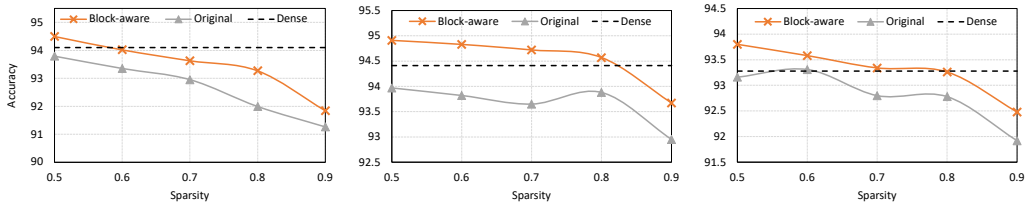

(a) WideResNet22-2 (b) ResNet18 (c) VGG16

Figure 14: Test accuracy (%) of shuffled-block dynamic sparse training with and without our block-aware drop criterion on CIFAR10.

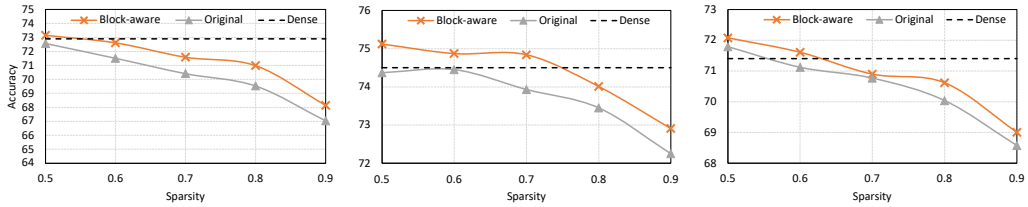

(a) WideResNet22-2 (b) ResNet18 (c) VGG16

Figure 15: Test accuracy (%) of shuffled-block dynamic sparse training with and without our block-aware drop criterion on CIFAR100.

avoid the computation of full gradients for model adaption. It computes the gradients for a superset of the active weights (with $ND + M$ parameters) in each iteration. After updating the $ND + M$ parameters, it selects ND parameters with the largest magnitudes from all parameters as the active weights for the next iteration. Thus, it needs to store all the N parameters. Compared to RigL and Top-KAST which needs to store either dense gradients or dense weights, our DSB stores sparse gradients and weights throughout the training process.

Table 3: Memory consumption of model weights and gradients with different sparse training methods. N is the number of parameters in the dense model, d represents the density of the sparse model, and M represents the extra number of gradients that need to be computed in Top-KAST. "Train" refers to the memory consumption in each training iteration, and "Model adaptation" refers to the memory used for adapting the sparse model.

	Train		Model adaptation	
	weights	gradients	weights	gradients
DSB	Nd	Nd	Nd	Nd
RigL	Nd	Nd	Nd	N
Top-KAST	N	$Nd + M$	-	-